Available online at www.eccomasproceedia.org
Eccomas Proceedia COMPDYN (2017) 3711-3727

ECCOMAS
Proceedia

COMPDYN 2017
6th ECCOMAS Thematic Conference on
Computational Methods in Structural Dynamics and Earthquake Engineering
M. Papadrakakis, M. Fragiadakis (eds.)
Rhodes Island, Greece, 15–17 June, 2017

DISSIPATING EFFECT OF GLAZED CURTAIN WALL STICK SYSTEM INSTALLED ON HIGH-RISE MEGA-BRACED FRAME-CORE BUILDINGS UNDER NONLINEAR SEISMIC EXCITATION

Lorenzo Casagrande[1,2], Antonio Bonati[1], Ferdinando Auricchio[2], Antonio Occhiuzzi[1]

[1] Construction Technologies Institute (ITC) - National Research Council (CNR)
viale Lombardia 49, MI 20098 ITALY
e-mail: {Casagrande,Bonati,Occhiuzzi}@itc.cnr.it

[2] University of Pavia - Civil Engineer and Architectural Department
via Ferrata 3, PV 27100 ITALY
e-mail: {Casagrande,Auricchio}@unipv.it

Keywords: High-rise Structures, Mega-braced Frames, Non-structural Elements, Glazed Curtain Walls, Nonlinear Dynamics, Earthquake Engineering

Abstract. *The results derived from the investigation on the dynamic behavior of glazed curtain wall non-structural stick systems installed in modern high-rise mega-frame prototypes is herein summarized. The supporting steel structures, designed in accordance with European rules, consisted of planar frames extracted from reference three-dimensional steel Moment Resisting Frame (MRF), respectively having thirty- and sixty-storey height. To limit interstorey drift and second order effects, outriggers trusses were placed every fifteen stories, whilst a CBF system was chosen as internal core. The characterization of non-structural façade elements was performed through experimental full-scale crescendo-tests on aluminium/glass curtain wall units. Deriving experimental force-displacement curves, it was possible to calibrate three-dimensional inelastic FE models, capable to simulate the interaction between glass panels and aluminium frame. Subsequently, equivalent nonlinear links were calibrated to reproduce the dynamic behaviour of tested glazed unit, and implemented in the thirty- and sixty-storey structural planar frames FE models. Nonlinear time history analyses (NLTHAs) were performed to quantify local and global performance, investigating the enhanced combination of stiffness and strength generated through the implementation of glazed curtain wall on the numerical FE models. Results will be shown in terms of inter-storey drift profiles and displacement peaks, axial force curves and percentage peak variation, showing the sensitivity to the structure height. Trends were discussed to show that, if accurately designed, omitting non-structural elements from the seismic assessment of high-rise prototypes conduct to a sensible underestimation of dynamic dissipation capacity of the building.*

Peer-review under responsibility of the organizing committee of COMPDYN 2017.
doi: 10.7712/120117.5677.17166

1 INTRODUCTION

Tall and super-tall buildings have become popular in urbanized areas due to the growing use of high-strength and smart materials, innovative construction techniques and cost effectiveness [1, 2, 3]. Moreover, the increasing demand for business and residential space have denoted the scarcity of land, constraining the wide use of high-rise structures in modern cities and facing relatively new criticalities, such as inappropriate ground typologies and areas of severe seismicity. Due to their intrinsic complex features and large dimensions [4, 5], several peculiar characteristics shall be considered during the design phase, ensuring the achievement of certain performance levels (i.e. collapse prevention, moderate damage, serviceability) and the evaluation of the characterizing mechanical aspects such as higher mode and longer periods in earthquake assessment [1, 6]. The strength decrease induced by geometric and material nonlinearities, local buckling or steel member fracture can lead to permanent damages or catastrophic collapses, while P-Δ effects can endanger such modern and more flexible buildings, posing challenges for seismic design in terms of stiffness and stability.

Generally, while mid-rise structures undergo to a combination of strength and stiffness design criteria, stiffness and stability usually govern the design phase in high-rise buildings. Since the design shall balance human safety and economic causes, governed by the variability of the background inputs and the structural assumptions, detailed analyses and ad-hoc studies are required to predict the seismic performance, such as scaled shaking table tests [7, 8] and advanced finite element (FE) simulations [1, 6]. The adoption of the performance-based design has shown that the synergy between structural and non-structural element performance becomes vital, since failure of architectural elements can decrease the performance level of the entire building. As observed during recent earthquakes, non-structural components represent the higher percentage in cost reparation, being the major initial investment. In particular, the large use of glazed curtain wall systems as external enclosures in high-rise modern buildings, has stimulated the researchers to examine the dynamic non-linear response of these non-structural elements. However, in comparison to structural elements, limited information has been collected on the dynamic design of non-structural members.

In light of this scenario, the present paper summarizes the results carried out through nonlinear modelling of high-rise moment resisting frame (MRF) steel systems: crescendo tests on full-scale glazed curtain wall system were performed to investigate to what extent façade elements affect structural frame global and local seismic response.

2 NONLINEAR DYNAMIC ANALYSES

In order to predict the dynamic behavior of the structural prototypes, nonlinear time history analyses (NLTHa) were performed, representing a robust and efficient tool to determine global and local seismic performances in structures. Since pushover analyses present specific limitations and inadequacies in high-rise MRFs design, principally the deficiency in safely estimation of the higher-mode effects in recent adaptive modal combinations (AMC) solutions [9, 10], nonlinear dynamic analyses have become the most attractive technique. Whereas different scale and peculiar responses of mechanical and physical idealizations are involved in façade-structure interaction, both detailed brick- and fiber-based FE models were assumed. On one hand, brick-based FE models give more knowledge on complex phenomena than equivalent mechanical representation [11, 12], being able to reproduce their local response in terms of time-dependent stress/strain concentration. On the other hand, the insight on the well-known physical phenomena allows their easy calibration into classical fiber-based FE models, saving

significant computational time. In this light, since a three-dimensional approach would be extremely onerous to investigate the full-scale mega-frame dynamic response, the contribution of the resisting frame system was easily incorporated into classical fibre force-based [13] FE models, able to represent bolted [14, 15, 16, 17, 18] and welded [11, 19, 20, 21] connections, and the other members besides. By contrast, aiming to develop a qualified façade numerical model and to understand the phenomena underpinning the mechanical global behavior, detailed brick-based FE simulations were performed in order to assess the aluminium frame deformability, the interaction between glass panels and aluminium frame, the gasket mechanical distortion and the transom-to-mullion connection stiffness. Finally, fiber-based link elements were calibrated from standard glazed curtain wall unit subjected to laboratory test and the relative three-dimensional FE model, in order to simulate their seismic response. In this scenario, the modeling assumptions and simulation techniques will be given, after a brief introduction on the main geometric and mechanical properties of both the examined planar frames and the tested façade.

2.1 Description of the case-study buildings

The two prototypes consisted on 6 x 6-bay buildings extracted from reference thirty- and sixty-storey three-dimensional structures, respectively named MF-01 and MF-02, designed in accordance with current European seismic standards [25] and considering high seismicity (i.e. PGA = 0.40 g) on soil class C (i.e. 180 m/s $<$ Vs $<$ 360 m/s).

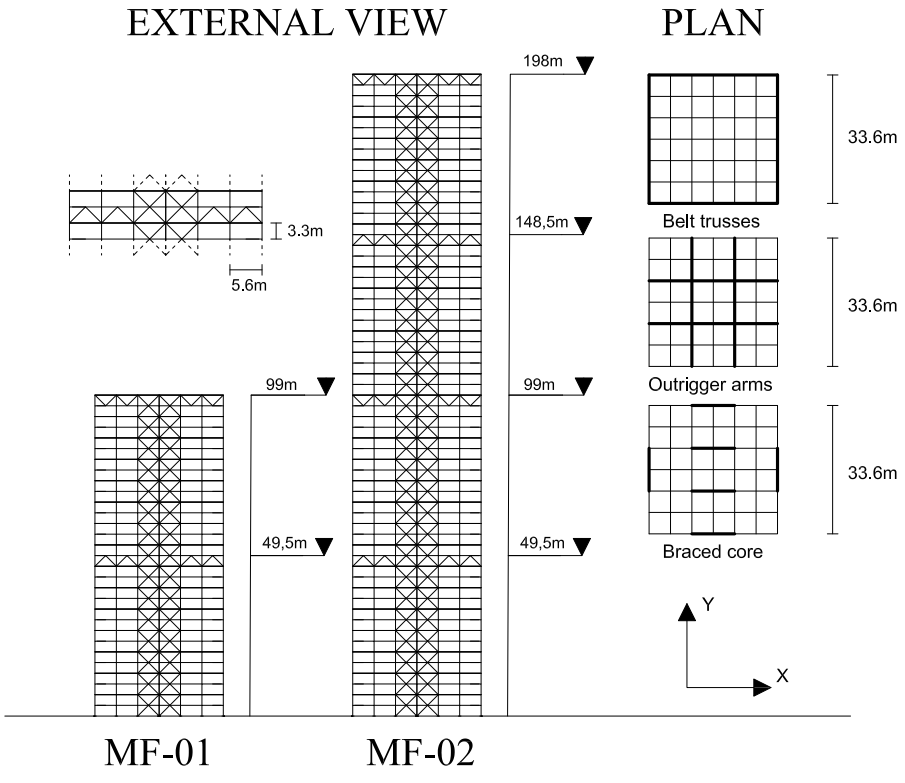

Figure 1: Structural scheme and geometric details of the reference thirty- and sixty-storey planar frames.

In addition to the permanent non-structural internal weight, dead and live loads were considered to be 2kN/m^2 and 4kN/m^2, respectively. According to ASCE-7 05 provisions [22], the lateral wind pressure was calculated considering the speed at the ground equal to 37 m/s (84

mph). The software used in the first-stage analyses and design were SAP 2000 [23] and MIDAS GEN [24], where a series of response spectrum analyses (RSAs) were performed on the MRF models. As shown in Figure 1, where a sketch of plan and elevation is provided, the complex lateral-force resisting system (LFRS) was constituted by a central 5.6 x 5.6m CBF core, connected with HD columns and perimetral CBF through one-storey height orthogonal outriggers, placed every fifteen stories to limit inter-storey drifts and second order effects. External belt trusses rang the structure. The behaviour factor (q) adopted for V bracing systems was conservatively assumed to be equal to 2, as specified in section 6.3 of EC8 [25], while medium ductility class (DCM) was considered according to EC8 prescriptions [25]. The beam span was set to 5.6 m, defining a uniform column spacing on the in-plane principal directions; accordingly with the tested façade geometry, the inter-storey height was set at 3.3 m, implying a global structural height of 99 m and 198 m for MF-01 and MF-02, respectively. Member sizes and mechanical properties adopted for the structural members were derived from the design phase, according to EC8 guidelines [25]. In detail, HD tapered profiles were used for the columns, while IPE400 beams were adopted for both prototypes in each storey, except for outrigger floors where HD steel sections were chosen. Hollow structural section (HSS) profiles were assumed as brace sections, decreasing in size along the height of the structure. According to [11], steel grade S275, S450 and S700 were used for beams, columns and braces, respectively. Figure 2 displays an example of welded gusset-plate and bolted beam-to-column connection. In Figure 2 (left), the HSS brace was welded to the gusset plate through fillet welds, while full penetration welds (FPW) were provided to connect the flanges of the columns and beams to the gusset plate.

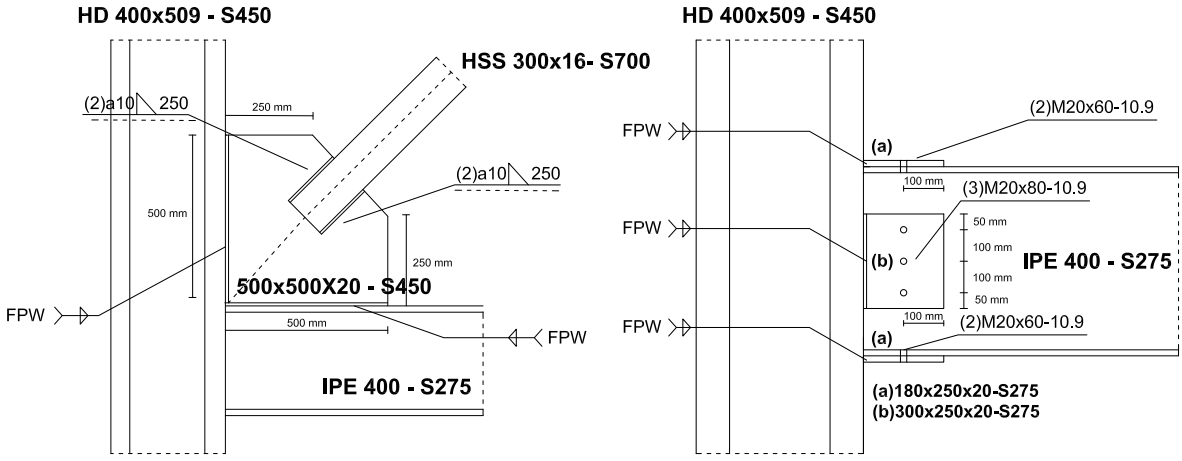

Figure 2: Example of designed gusset-plate (left) and beam-to-column (right) connections.

Furthermore, gusset plate design for each storey in MF-01 and MF-02 prototypes, was performed according to the prescription in [25, 11]. Figure 2 (right), shows the partially-restrained joint obtained through two M20x80-10.9 bolts used to connect the flange of the beam to a 180x250x20 mm plate, welded by FPW to the flange of the column in accordance with the prescriptions of [19]. Three M20x80-10.9 bolts were used to bolt the web of the beam to the shear tab. In the end, the structure was considered to be fixed to the ground, both during the design process and the numerical simulations. The fundamental period (T1) was determined to be equal to 1.75 s for MF-01 and 4.16 s for MF-02 prototypes.

2.2 Description of the test performed on the commercial stick curtain wall

This paper focuses on previously performed experimental data, achieved by full-size in-plane tests led at the laboratory of the Construction Tecnologies Institute (ITC) of the Italian National Research Council (CNR) [26]. The seismic response of a commercial full-scale stick curtain wall was evaluated, comparing the integrity of results with past studies [27, 28, 29, 30, 31].

2.2.1 Experimental setup and equipment

The experimental setup consisted in a 5.720 x 7.370 mm steel frame, where three rigid beams were installed at different height, representing the principal structure slabs and adaptable to different curtain wall geometries. Furthermore, horizontal displacement could be imposed to the rigid beams in order to simulate seismic-induced lateral drifts [32, 33]; however, during the test only the median beam was activated, while the upper and lower beam were rigidly fixed to the supporting frame. In particular, a hydraulic actuator (General Hydraulic, stroke $\pm$ 600mm, maximum load 200 kN) was fixed to an external rigid reaction system and pushed in the horizontal in-plane direction, in correspondence to the beam-mullion connection, performing the force-control test. The instrumentation was composed by a 50 kN LeBow load cell, capable to measure the applied force, and two linear potentiometric displacement transducers (LVDT) to measure horizontal displacement of the median beam; a 10 Hz continuous data acquisition collected load and displacement during the tests. Figure 3 shows the test set-up and the aluminium member cross-section geometries.

2.2.2 Description of the façade specimen

Consistently with the designed mega-frame steel structure geometry, the investigated façade was 7200 mm high and 5600 mm wide, with 3300 mm inter-storey height. The test unit had six transoms and five mullions, while three different profile cross-sections were used for mullions and three for transoms (Figure 3). In particular, transoms of the external bays displayed a cross-section with lower inertia respect to the other spans. EN-AW 6060-T6 was the commercial aluminium alloy adopted for the members, with E = 69 GPa as Young Modulus, σ_y = 150MPa and σ_u = 190MPa as yield and ultimate stress. The insulated glazing panel thickness was 8+8.2+16+6mm, constituted by a tempered glass characterized by E = 70 GPa and supported on the edges by silicone gaskets. Two mechanical connections were recognizable into the test unit: the transom-to-mullion and the glass-to-frame connection. The former, realized by a U-shaped steel joint, was connected to the alluminium members by four steel screws, resulting in a reduced rotational stiffness with respect to the fully-fixed configuration. The latter, was obtained distributing an internal and external silicone gaskets layer along the contact edges. The clearance between the mullion/transom elements and the glass panels was 5mm.

2.2.3 Experimental activity and results

Initially, a quasi-static test was performed increasing the force applied to the central rigid beam until a specific drift was monitored on the opposite mullion. Consequently, the force was set to zero, highlighting the amount of residual plastic deformations. Since the specimen had an opening window impossible to re-close after the first cycle, due to the shear deformations of the frame, the subsequent cycles were performed with opened window. However, repeating the first cycle was possible to observe the incidence of a single window loss, showing that the missing

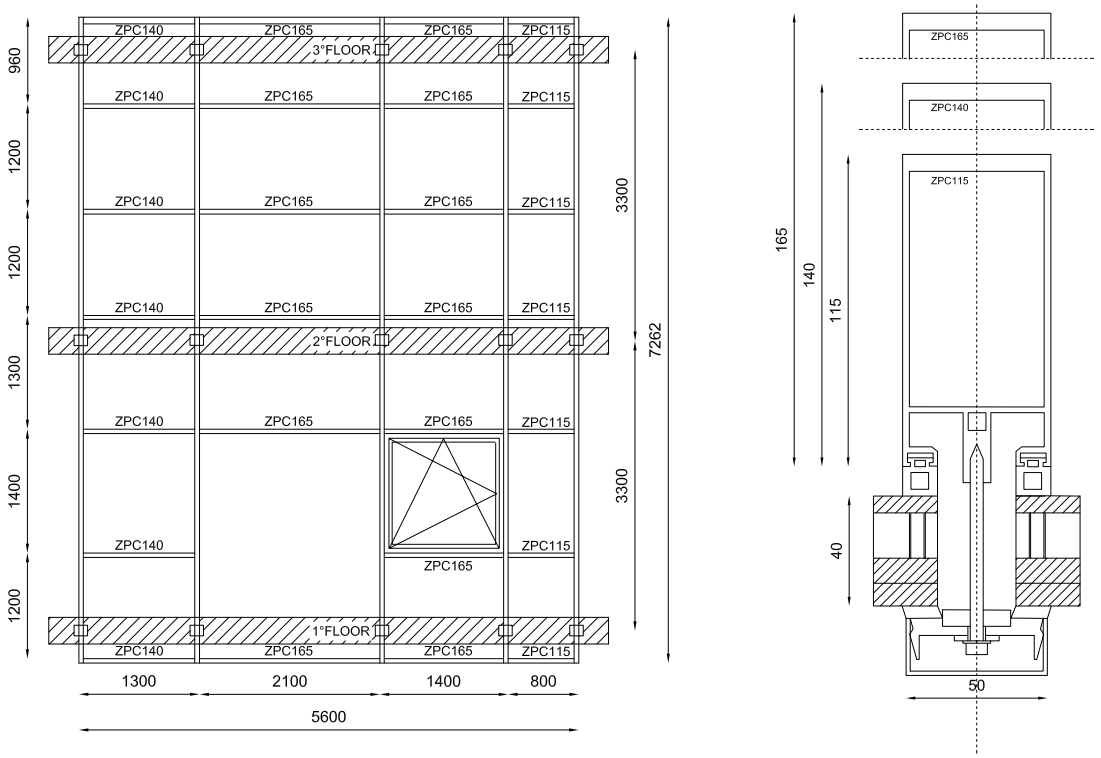

Figure 3: Façade geometry (left) and transom/mullion cross-sections (right). Note: dimensions in mm.

glass panel did not modified the façade response. The force-to-drift results are displayed in Figure 8, in accordance with Caterino et al. [26].

2.3 Finite Element modelling approach

In order to investigate the effect of glazed curtain walls on structural seismic behavior when applied to mega-tall buildings, a three-stages FE modeling approach was implemented. First-stage modelling aimed to reproduce nonlinear fibre-based simulations of the building case-studyies, subjected to NLTHAs deriving from a set of ten natural records [34, 35]. These accelerograms (EQs) were spectrum-compatible in displacement according to EC8 prescriptions [25], selected a Type 1 spectrum with PGA equal to 0.4g, soil Type C and T_D=8s (Figure 4). Second-stage advanced modelling investigated the dynamic behaviour of the façade through nonlinear brick-based models, simulating the test results. Finally, third-stage modelling aimed to calibrate equivalent nonlinear links, representing the glazed curtain wall response to be implemented on first-stage fibre-base FE models.

2.3.1 Fibre-based modelling approach for MRF structure

In order to analyze the local and global seismic response of the MF-01 and MF-02 reference structures, detailed fiber-based models were implemented on the open source platform OpenSees [36], based on conceptual modeling by Brunesi et al. [42]. Structural members were modeled through inelastic force-based fiber elements, simulating the propagation of inelasticity over the member length through a bilinear stress-strain behavior with isotropic strain hardening. In particular, the Menegotto-Pinto [37] material model was adopted, while material and geometrical nonlinearities were considered through distributed plasticity approach and classi-

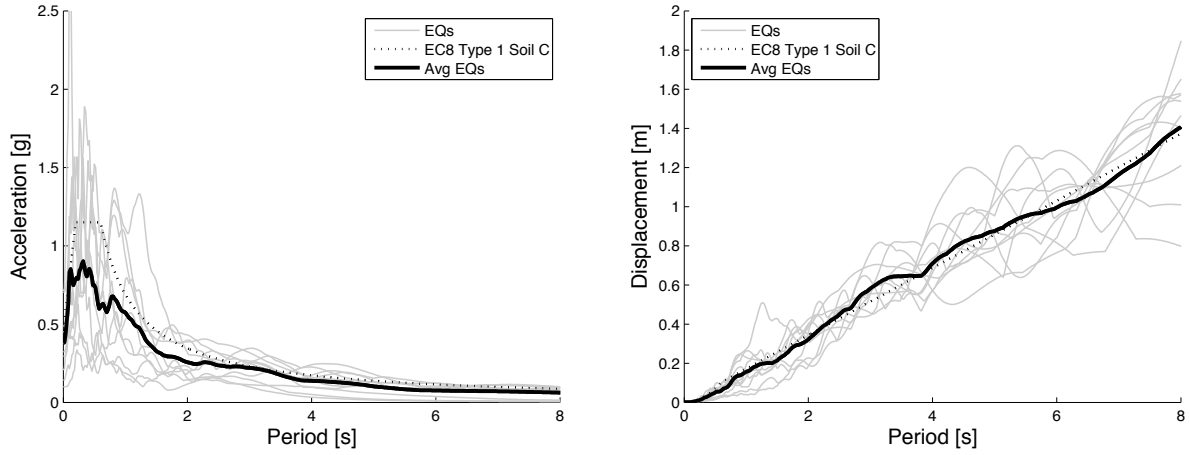

Figure 4: Seismic input as acceleration (left) and displacement (right) elastic response spectra.

cal corotational transformation [38]. Schematics of the modelling idealization adopted for brace and gusset plate mechanical connections are showed in Figure 5. The enhanced stiffness due to the gusset-plate welding into the beam-column conjunction, that confine the extremity of inelastic force-based beam-column portions, was adduced introducing a set of rigid elements [11, 19]. Along the end of the brace, in order to capture the potential progression of plastic hinges, an additional $2t$-length force-based beam-column element was selected from the gusset plate - where t is the thickness of the gusset plate - [11, 19, 43]. Prospective buckling mechanisms in both braces and gusset plates were considered applying an out-of-plane imperfection equal to 0.1% of the length at its midspan. Similarly, according to [12, 14, 15, 16, 18, 39, 40, 42], the T-stub bolted joint mechanical idealization was assumed to reproduce the hysteresis behavior, as a partially restrained connection. Accordingly to the Grant and Priestley paradigm [41], when considering the tangent stiffness-proportional Rayleigh damping, the stiffness-proportional matrix multiplying coefficient used to perform nonlinear dynamic analyses was correlated to the damping ratio associated to the fundamental period of the structure [38, 41, 42, 43].

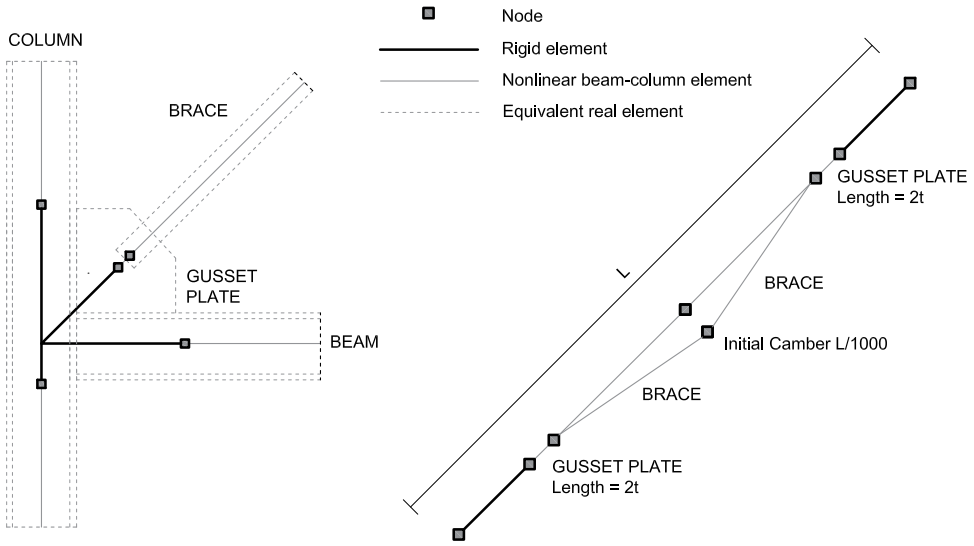

Figure 5: Modeling idealization for brace and gusset-plate connections.

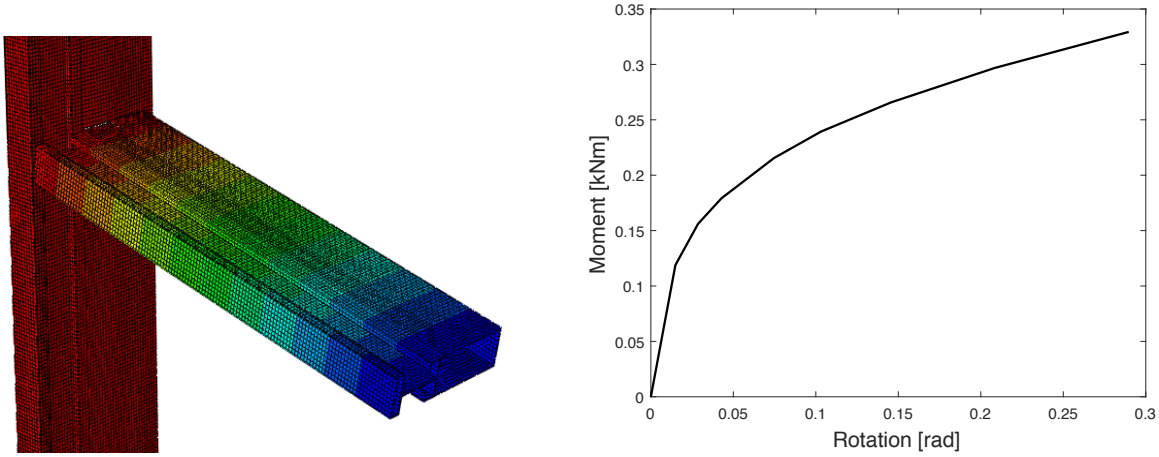

Figure 6: Three-dimensional modelling (left) and moment-rotation diagram (right) of the transom-to-mullion connections.

2.3.2 Three-dimensional solid-based modelling approach for façade

Advanced numerical simulations were performed to reproduce the dissipative behavior of the tested glazed curtain wall unit. In particular, four parameters were recognized as main responsible of the lateral response of the façade: *(i)* the geometry of aluminium frame and the rotational stiffness of transom-to-mullion connections; *(ii)* the clearance between aluminium frame and glass panels; *(iii)* the mechanical behavior of gaskets; *(iv)* the local interaction between glass and frame [32, 33, 31]. Three-dimensional brick-based models were analysed in ABAQUS 6.14 [44] in order to capture the local mechanisms and the interactions between each parameter affecting the overall response. Therefore, equivalent nonlinear link-elements were calibrated to explicitly reproduce the rotational stiffness of transom-to-mullion connections and the combined effect of glass-to-gaskets slippage, considering potential impacts between the glazed surface and the aluminium frame, as in Figure 6-7, in line with a computational time-saving approach [45, 46]. In fact, these connectors were implemented on a full-scale model, as on Figure 8, reducing the FE formulation variables and reproducing the global tested response.

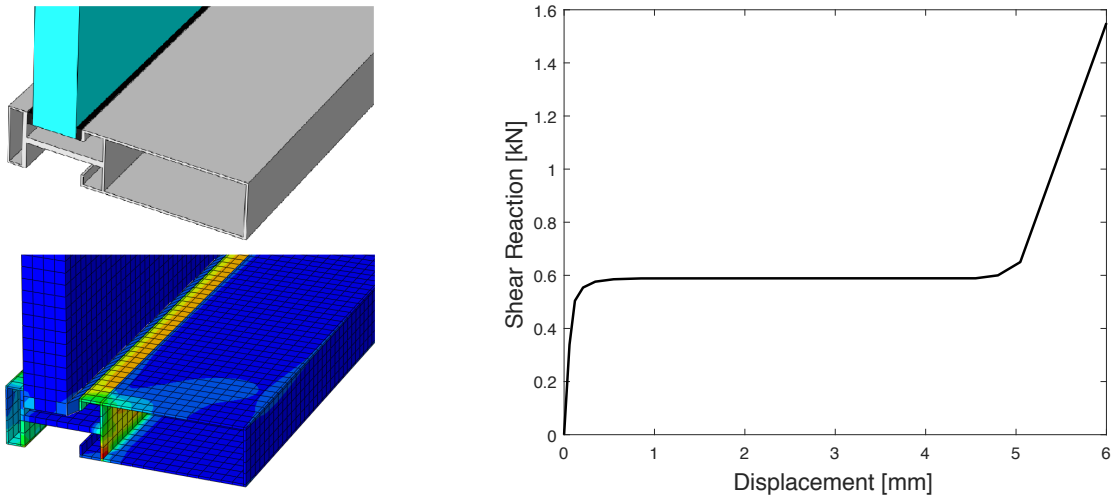

Figure 7: Three-dimensional modelling (left) and shear-displacement diagram (right) of the glass-to-gasket connections.

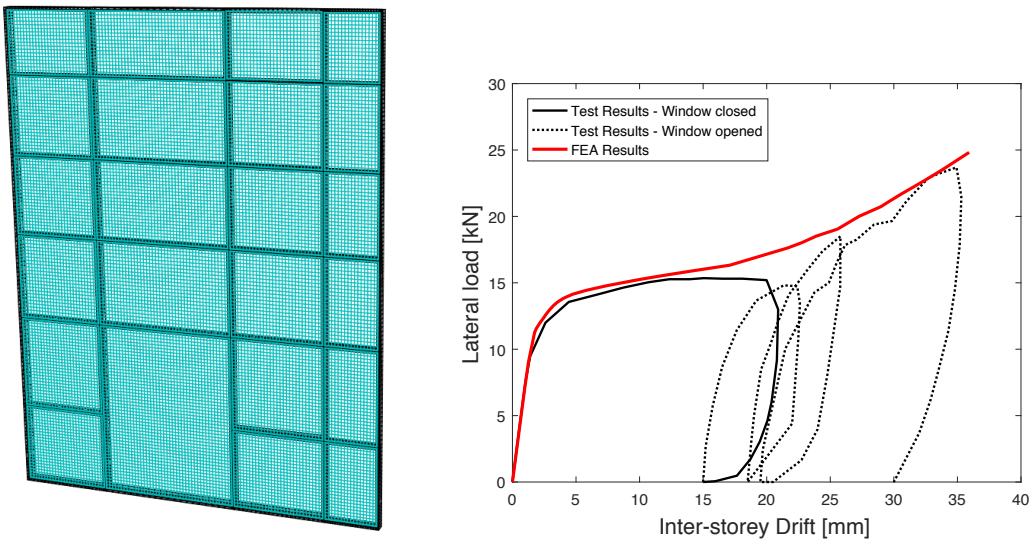

Figure 8: Three-dimensional modelling (left) and force-displacement diagram (right) of tested façade.

Figure 6 displays a high-fidelity FE model calibrated to investigate the moment-rotation relationship of transom-to-mullion connection. Three-dimensional deformable isoparametric solids were adopted to model each connection component, accounting for finite strain and rotation in large-displacement analysis. Fist-order elements were adopted, i.e. 8-node linear brick (C3D8R), with reduced integration through Barlow points and hourglass control methods of Flanagan and Belytschko. Both geometrical and material nonlinearities were considered. The classical rate-independent Von Mises model for metal plasticity with associated yield surface for isotropic materials and strain hardening was assumed to faithfully reproduce the cyclic stress-strain relationship of the steel members during the applied loading-unloading history. Since the U-shaped connecting steel joint presented higher stiffness and strength respect to the aluminium members, it was considered that the joint rotational capacity was mainly due to the deformation of the frame. Therefore, the simulation remained accurate properly representing bolted connections through equivalent nonlinear frictional parameters and constraining the effect of slipperiness between the U-shaped joint and the aluminum members. Figure 7 presents a robust brick-based FE modeling developed to study the glass-to-gaskets interaction, at a local scale. While the same mechanical and physical assumptions for aluminum members were considered, the constitutive laws for glass and gaskets were herein introduced. According to Memari et al. [46], the glass panel was considered as an equivalent full-section isotropic elastic three-dimensional element (C3D8R), evaluating the maximum stress response. The glass-to-gasket nonlinear friction effect and the mechanical deformation of the gasket were modeled by elasto-plastic relationship with isotropic hardening, connecting the nodes on the glass panel boundary to the the frame nodes. The calibration of the equivalent stress-strain constitutive laws was conducted in accordance with [46, 47, 48] and the experimental tests carried out at the Institute of Construction Technology. Since numerous in-plane racking tests [29, 45, 46] have shown that glass damage propagates when glass-to-frame contact occurs along glass-panel edges in corner regions, the stiffening interaction due to the impact was directly incorporated onto gasket constitutive laws, through a validated parametric campaign of FEM analyses. Figure 8 shows the advanced three-dimensional modeling of the tested façade and the accurate matching between the simulation and experimental results. Equivalent nonlinear links were calibrated to represent the seismic response of the glazed curtain wall in OpenSees high-rise reference structures.

3 RESULTS AND COMPARISONS

In this chapter, the main results will be displayed in terms of NLTHa global and local performance, of the two reference high-rise structures MF-01 and MF-02. In particular, the influence of the glazed curtain wall system will be shown, illustrating to which extent this affects the overall seismic response when façades are considered acting on the LFRSs. Initially, each section will display the comparison between NLTHa average response (NLTHA Avg), carried out from the structures with glazed curtain walls, respect to the correspondent bare MRF. Consequently, the percentage variation between both component will be shown. Individual earthquake (EQs) acceleration result, referred to the MRF with non-structural elements, will be shown in grey.

3.1 Global performance

Figure 9 summarizes the global response of the two mega-frame buildings in terms of peak displacement and inter-storey drift, together with their average values, respectively for MF-01 (left) and MF-02 (right). Peak displacements, achieved in the most extreme records, were 0.58 m and 1.72 m, while medium values up to 0.41 m and 0.88 m were obtained. The response assumed a rough cantilevered shape with soft discrepancy in correspondence to the outrigger; as will be discussed in the following, this aspect was more pronounced in the inter-storey drift prediction (Figure 9).

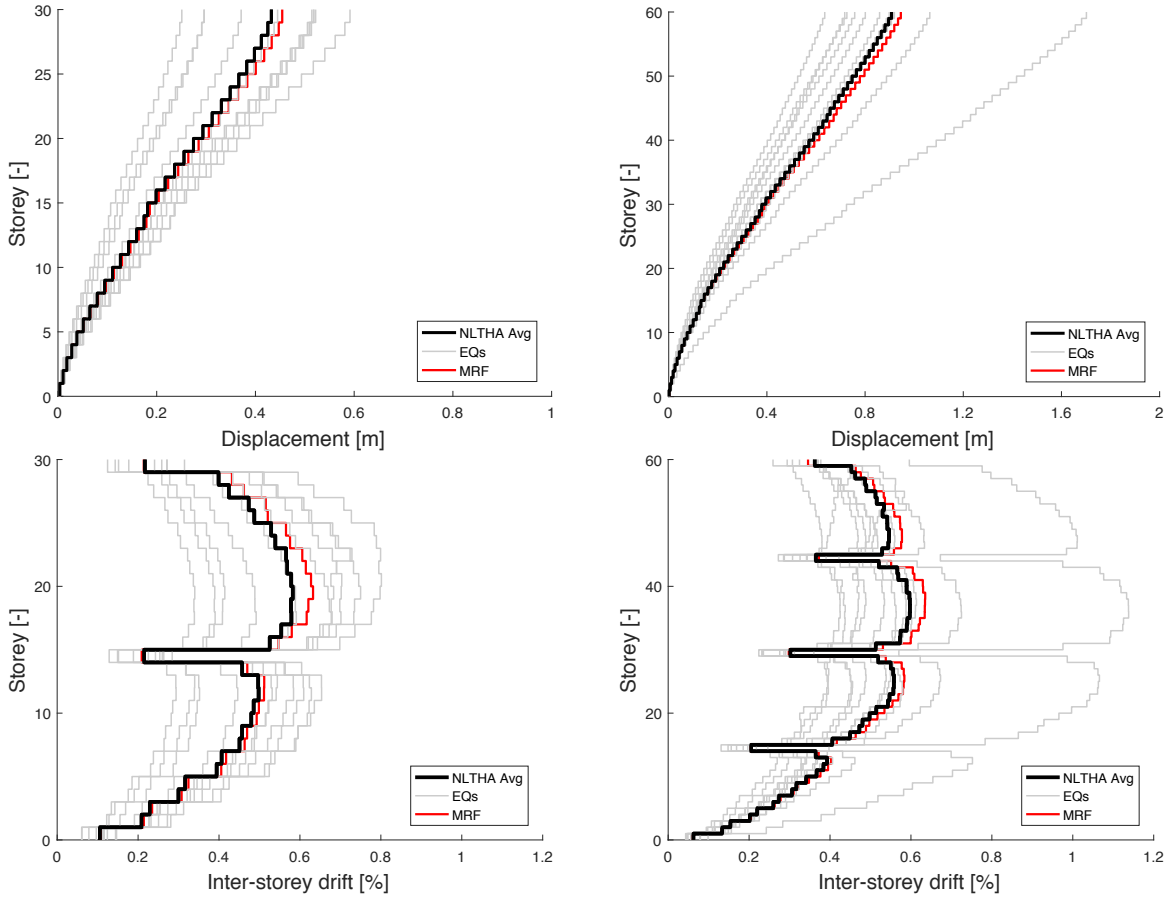

Figure 9: Displacement profile and Inter-storey drift of MF-01 (left) and MF-02 (right).

The stiffening enhancement procured by the outriggers was significantly visible for both structure, as a prominent peak inter-storey drifts reduction (up to 57%). By contrast, significant

acceleration were experienced during dynamic simulations, i.e. 0.59g and 0.35g for both MF-01 and MF-02, respectively, underlining the stiffest behavior of the former (as also evidenced by fundamental periods discrepancy, i.e. 1.75 s vs. 4.16 s). The series of NLTHa have shown that, if properly designed to induce a good balance between acceleration and deformation demands, this structural system supply an optimum combination of global stiffness and strength in high-rise structures. Moreover, since MRF contribution was greater than NLTHA Avg (Figure 9), this illustrates that the MRF structure was more flexible without considering the external façades.

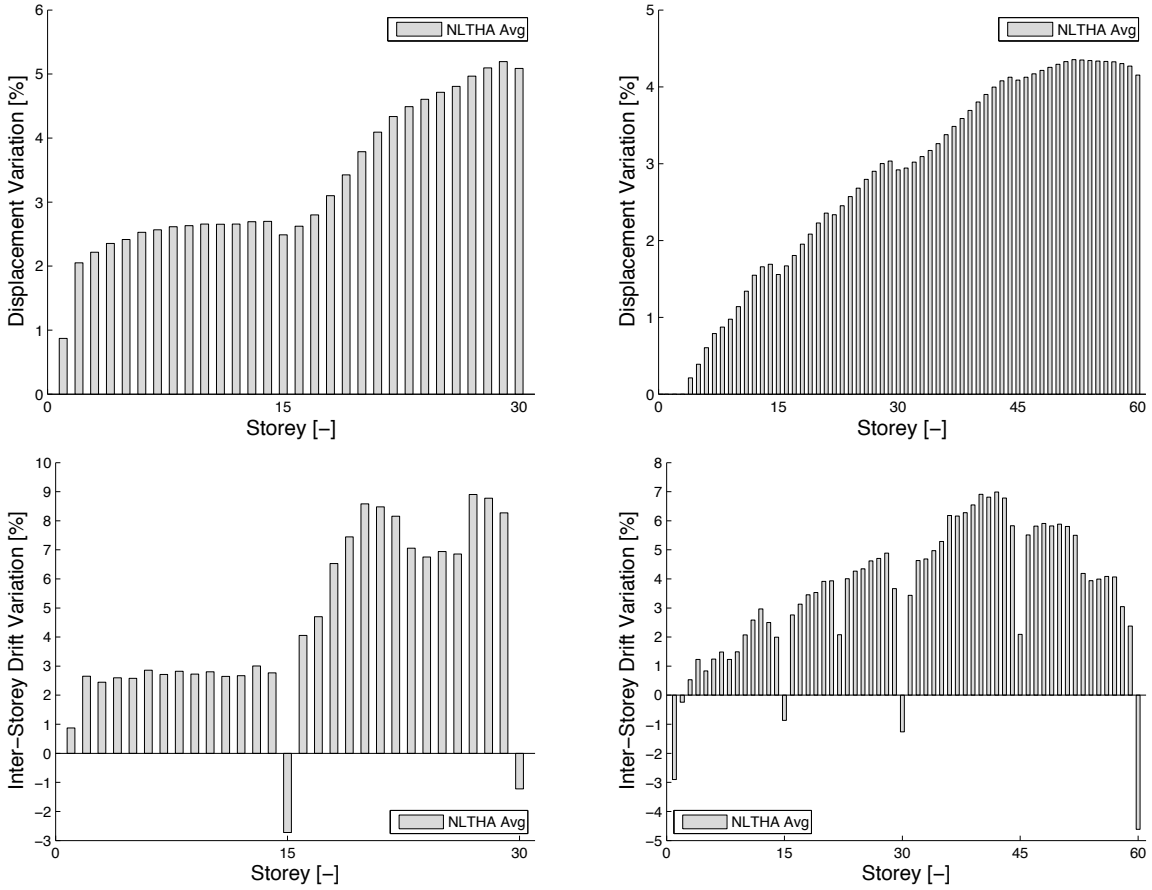

Figure 10: Displacement profile and Inter-storey drift variation of MF-01 (left) and MF-02 (right).

In fact, Figure 10 shows to what extent the variation between the overall structural response of the MRF with glazed façades differed from the bare MRF. Peak discrepancies were accounted for 5.45% and 4.53% as top average displacement, respectively for MF-01 and MF-02, while 9.23% and 7.47% represented the inter-storey drift profile in average. The shape of the displacement variation reflected the tendency of the displacement diagram, assuming a fairly-cantilevered progression. It was clearly visible the outrigger influence in inter-storey drift profiles, showing a trend reversal, while on the displacement variation profile the effect attenuates.

3.2 Local performance

According to Brunesi et al. [42, 43], the key components advocated to resist seismic actions in this structural system are columns, braces and outriggers. Response in term of axial load peak profiles in critical members will be shown. In addition, the percentage variation between the MRF with external cladding and bare MRF results will be computed.

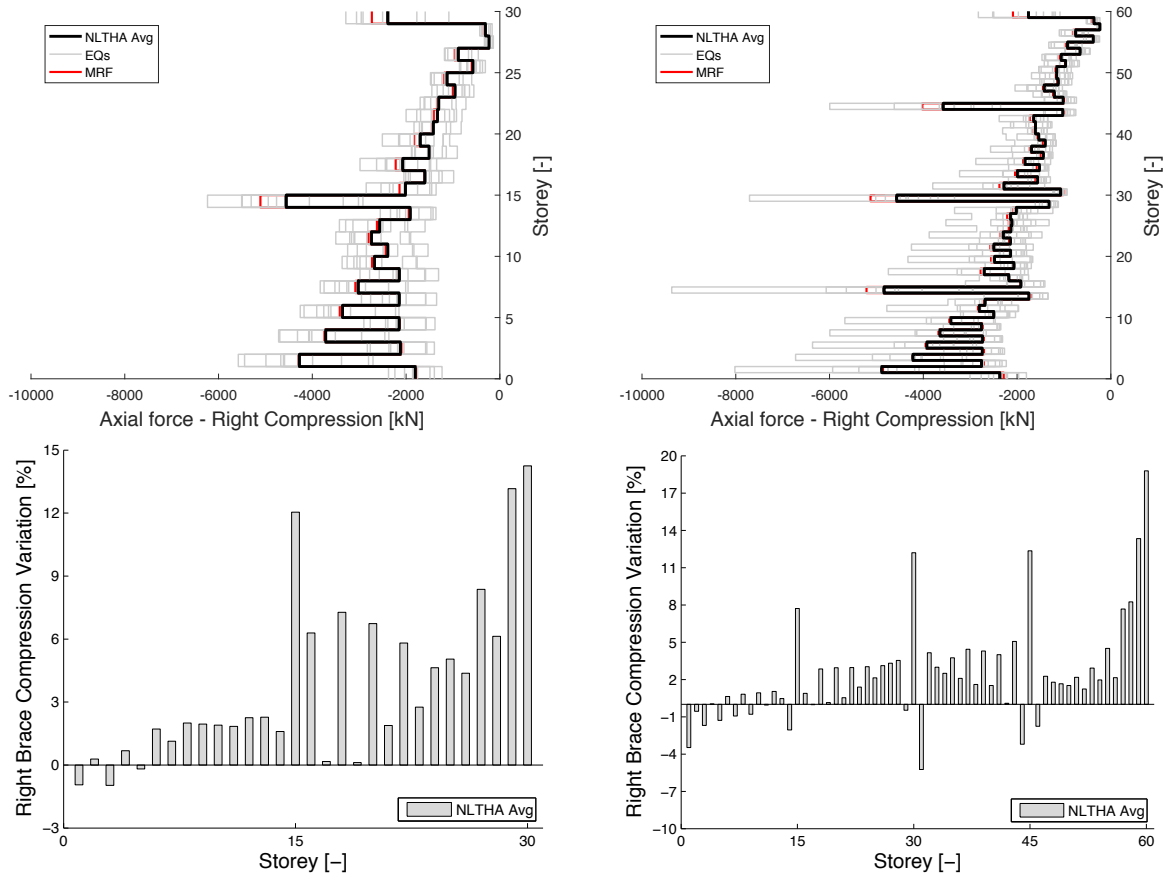

Figure 11: Axial force profile in reference braces and compression variation, in MF-01 (left) and MF-02 (right).

In Figure 11 the comparison between compressive peak forces in the most critical brace is displayed. Average loads of up to 4500 kN and 5000 kN were obtained, respectively for MF-01 and MF-01. A similar demand was obtained in correspondence to the outriggers floors, as a consequence of the increment in terms of floor acceleration [42, 43], where was demonstrated that modelling the structure without the curtain walls conduced to overestimate NLTHAs results up to 20%. Figure 12 summarizes the seismic peak axial loads predicted by NLTHAs in the outrigger braces, placed at the 15^{th} and 30^{th} storey of the thirty- and sixty- storey case study building, since they resulted to be the most critical storeys (see Figure 11). The diagrams present a comparison between the forces observed considering the MRF with the external façade and the supporting structure alone: peak compression was almost stable along the height, reaching a maximum of 4250kN and 4500kN, in MF-01 and MF-02, respectively. However, a larger mismatch between axial force percentage variation was determined in the outriggers placed at the top of MF-01 and at mid-height of MF-02, of up to approximately 25%. Being the discrepancy between the response of MRF with cladding and the bare MRF higher in that braces than that observed in other structural members, particular care has to be paid to the earthquake-induced demand evaluation during the design phase of these elements and the related connections. As a result of the outriggers in-plane rotation, earthquake-induced compressive overloads were experienced by the external core-columns [42, 43]. Figure 13 collects the seismic axial forces transferred to the leftmost core-column of the thirty- and sixty-storey structures, accounting for the façade system, their average and the equivalent on the bare MRF. This reflected on the discrepancy between forces, up to approximately 14% in MF-01 and 18% in MF-02.

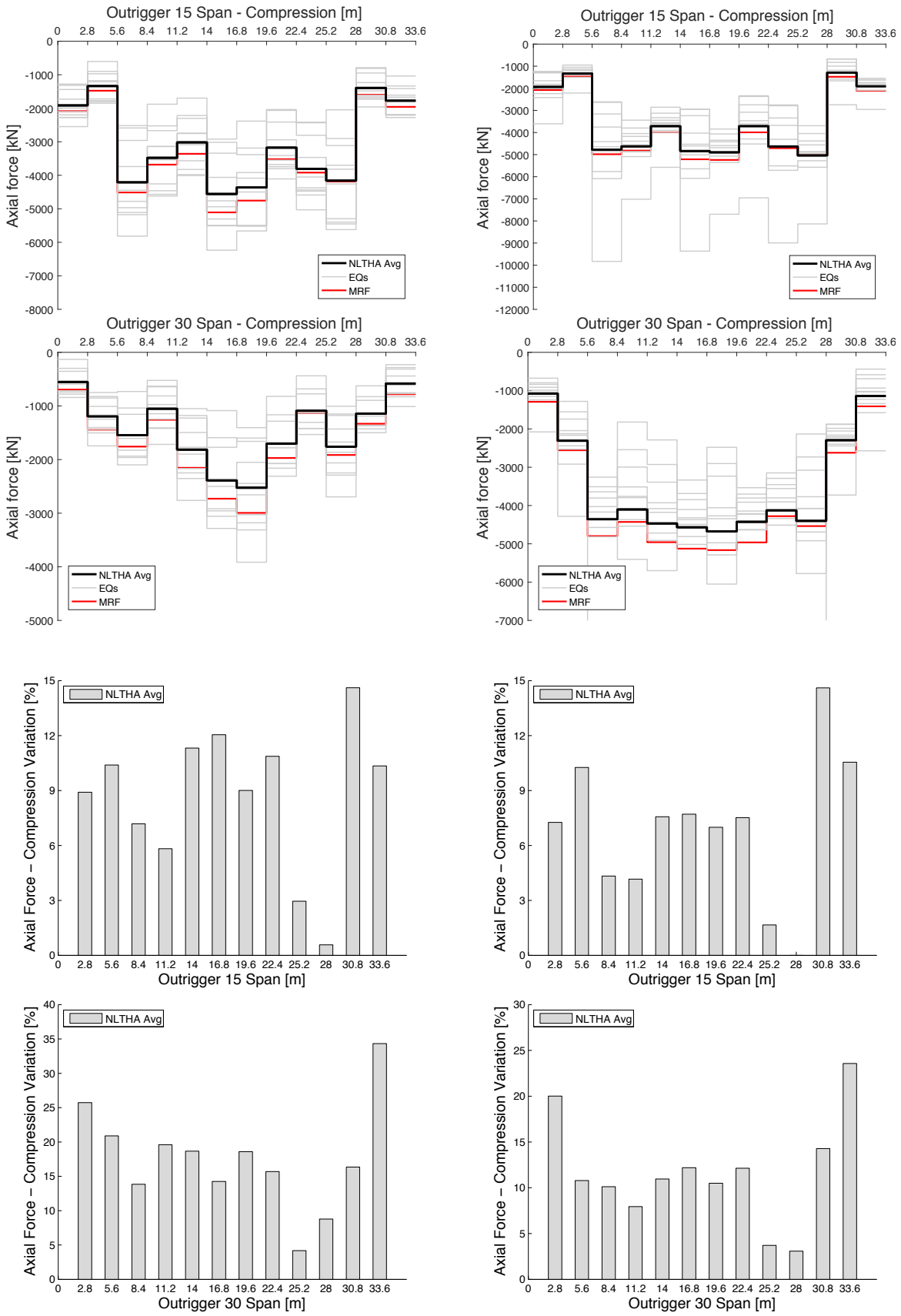

Figure 12: Axial force profile in outrigger braces and compression variation, in MF-01 (left) and MF-02 (right).

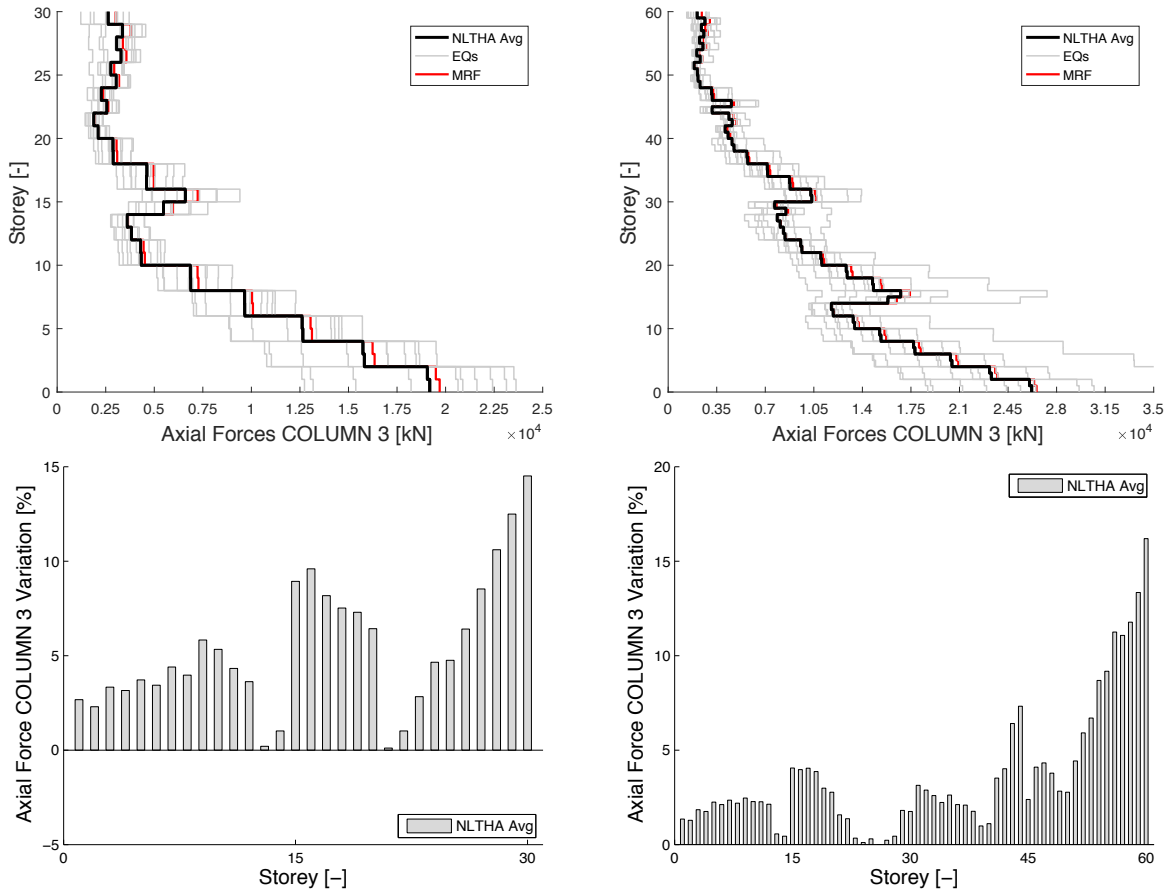

Figure 13: Axial force peak profile in the lefmost core column and compression variation, in MF-01 (left) and MF-02 (right).

4 CONCLUSIONS

This paper summarizes the NLTHAs results performed on two reference thirty- and sixty-storey planar prototypes, extracted from a high-rise mega-braced frame structures with outriggers and belt trusses, and designed according to European prescriptions. In detail, the research focuses on the dynamic of glazed curtain walls, i.e. to what extent is plausible consider façades interacting with the LRFS during a severe earthquake event, altering the structural seismic response. The main observations acquired from the numerical analysis results are synthesized:

- Effects caused by façade dissipation were proven to be not negligibly on the LRFS and on the key components of both prototypes, reflecting dissimilarities up to 9.23% and 34.2% as local and global response, respectively. Fundamental period decremented up to 14.3% in MF-01 and 11.3% in MF-02, considering the glazed curtain wall dissipation.
- Response profiles and peak variations were characterized by an approximately linear increasing trend along the height, with pronounced discontinuities in correspondence to the outriggers, due to their overall stiffening effect.
- External outrigger braces resulted to be the most influenced by the cladding dissipation.
- Sensitivity to the structure height was investigated as a result of glazed curtain wall response, showing that façades mainly influence global and local response with a reverse fashion respect to the structural height.

REFERENCES

[1] H. Fan, Q.S. Li, A.Y. Tuan, L. Xu, Seismic analysis of the world's tallest building, *J Constr Steel Res 2009*, **65**, 1206-15.

[2] X. Lu, X. Lu, H. Guan, W. Zhang, L. Ye, Earthquake-induced collapse simulation of a super-tall mega-braced frame-core tube building, *J Constr Steel Res 2013*, **82**, 59-71.

[3] X. Lu, X. Lu, H. Sezen, L. Ye, Development of a simplified model and seismic energy dissipation in a super-tall building, *Eng Struct 2014*, **67**, 109-22.

[4] G.M. Montuori, E. Mele, G. Brandonisio, A. De luca, Secondary bracing systems for diagrid structures in tall buildings, *Eng Struct 2014*, **75**, 477-88.

[5] G.M. Montuori, E. Mele, G. Brandonisio, A. De luca, Design criteria for diagrid tall buildings: stiffness versus strength, *Struct Des Tall Spec Build 2014*, **23**, 1294-314.

[6] T.S. Jan, M.W. Liu, Y.C. Kao, An upper-bound pushover analysis procedure for estimating the seismic demands of high-rise buildings, *Eng Struct 2004*, **26**, 117-28.

[7] C.S. Li, S.S.E. Lam, M. Z. Zhang, Y. L. Wong, Shaking table test of a 1:20 scale high-rise building with a transfer plate system, *J Struct Eng ASCE 2006*, **132**, 1732-44.

[8] X.L. Lu, Y. Zou, W.S. Lu, B. Zhao, Shaking table model test on Shangai world financial center tower. *Earthq Eng Struct Dyn 2007*, **36**, 439-57.

[9] H. Krawinkler, G.D.P.K. Seneviratna, Pros and cons of pushover analysis of seismic performance evaluation, *Eng Struct 1998*, **20**, 452-62.

[10] A.K. Chopra, R.K. Goel, A modal pushover analysis procedure to estimate seismic demand for unsymmetric-plan buildings, *Earthq Eng Struct Dyn 2004*, **33**, 903-27.

[11] R. Nascimbene, G.A. Rassati, K.K. Wijesundara, Numerical simulation of gusset-plate connections with rectangular hollow section shape brace under quasi-static cyclic loading, *J Constr Steel Res 2011*, **70**, 177-79.

[12] E. Brunesi, R. Nascimbene, M. Pagani, D. Belic, Seismic performance of storage steel tanks during the May 2012 Emilia, Italy, earthquakes, *J Perform Constr Fac ASCE 2015*, **29**(5), 04014137.

[13] E. Spacone, F.C. Filippou, F.F. Taucer, Fibre beam-column model for non-linear analysis of RC frames: Part 1. Forumlation, *Earthq Eng Struc Dyn 1996*, **25**, 711-25.

[14] E. Brunesi, R. Nascimbene, G.A. Rassati, Response of partially-restrained bolted beam-to-column connections under cyclic loads, *J Constr Steel Res 2014*, **97**, 24-38.

[15] E. Brunesi, R. Nascimbene, G.A. Rassati, Evaluation of the response of partially restrained bolted beam-to-column connection subjected to cyclic pseudo-static loads, *Structure Congress, Pittsburg, Pennsylvania, May 2-4, 2013*, p. 2310-21.

[16] E. Brunesi, R. Nascimbene, G.A. Rassati, Seismic response of MRFs with partially-restrained bolted beam-to-column connections through FE analyses, *J Constr Steel Res 2015*, **107**, 37-49.

[17] E. Brunesi, R. Nascimbene, G.A. Rassati, Seismic performance of steel MRF with partially-restrained bolted beam-to-column connections through FE simulations, *Structures Congress 2014, Boston, Massachussets, April 3-5, 2014*, p. 2640-51.

[18] G.A. Rassati, R.T. Leon, S. Noe, Component modeling of partially restrained composite joints under cyclic and dynamic loading, *J Struct Eng ASCE 2004*, **130**, 343-51.

[19] S. Santagati, D. Bolognini, R. Nascimbene, Strain life analysis at low-cycle fatigue on concentrically braced steel structures with RHS shape braces, *J Earthq Eng 2012*, **16**, 107-37.

[20] K.K Wijesundara, R. Nascimbene, T.J. Sullivan, Equivalent viscous damping for steel concentrically braced frame structures, *Bull Earthq Eng 2011*, **9**, 1535-58.

[21] K.K Wijesundara, R. Nascimbene, G.A. Rassati, Modeling of different bracing configurations in multi-storey concentrically braced frames using a fiber-beam based approach, *J Constr Steel Res 2014*, **101**, 426-36.

[22] ASCE 7-05. Minimum design loads for buildings and other structures, *Reston (VA): American Society of Civil Engineers 2006*.

[23] SAP2000. Linear and nonlinear static and dynamic analysis and design of three-dimensional structures, *Berkeley (CA): Computers and Structures Inc. (CSI)*.

[24] MIDAS GEN: Integrated Design system for Buildings and General Structures, *Korea: MIDAS Information Technology Co., Ltd.*.

[25] Eurocode 8. Design of structures for earthquake resistance - Part 1: General rules, seismic actions and rules for buildings, *EN 1998-1-1. Brussels (Belgium) 2005*.

[26] N. Caterino, M. Del Zoppo, G. Maddaloni, A. Bonati, G. Cavanna, A. Occhiuzzi, Seismic assessment and finite element modelling of glazed curtain walls, *Struct Eng and Mech 2017*, **61**(1), 77-90.

[27] S.J. Thurston, A.B. King, Two-directional cyclic racking of corner curtain wall glazing, *Building Research Association of New Zeland (BRANZ) 1992*.

[28] C.P. Pantelides, R.A. Behr, Dynamic in-plane racking tests of curtain wall glass elements, *Earthq Eng Struc Dyn 1994*, **23**(2), 211-228.

[29] R.A. Behr, A. Belarbi, J.H. Culp, Dynamic racking tests of curtain wall glass elements with in-plane and out-of-plane motions, *Earthq Eng Struc Dyn 1995b*, **24**(1), 1-14.

[30] R.A. Behr, Seismic performance of architectural glass in mid-rise curtain wall, *J Arch Eng 1998*, **4**(3), 94-98.

[31] H. Sucuoĝlu, C.G. Vallabhan, Behaviour of window glass panels during earthquakes, *Eng Struc 1997*, **19**(8), 685-694.

[32] J.G. Bouwkamp, J.F. Meehan, Drift limitations imposed by glass, *Proceedings of the Second World Conference on Earthquake Engineering, Tokyo, Japan, 1960*.

[33] J.G. Bouwkamp, Behavior of windows panels under in-plane forces, *Bull Seism Soc Am 1961*, **51.1**, 85-109.

[34] T.J. Sullivan, Direct displacement-based seismic design of steel eccentrically braced frame structures, *Bull Earthq Eng 2013*, **11**, 2197-231.

[35] T.J. Maley, R. Roldán, A. Lago, T.J. Sullivan, Effects of response spectrum shape on the response of steel frame and frame-wall structures, *Pavia (Italy): IUSS Press 2012*.

[36] OpenSees. Open system for earthquake engineering simulation, *Berkeley (CA): Pacific Earthquake Engineering Research Center, University of California*.

[37] F.C. Filippou, E.P. Popov, V.V. Bertero, Effects of Bond Deterioration on Hysteretic Behavior of Reinforced Concrete Joints *Earthquake Engineering Research Center, University of California, Berkeley 1983*, Report EERC 83-19.

[38] E. Brunesi, R. Nascimbene, Extreme response of reinforced concrete buildings through fiber force-based finite element analysis, *Eng Struct 2014*, **69**, 206-15.

[39] A. Braconi, W. Salvatore, R. Tremblay, O.S. Bursi, Behaviour and modelling of partial-strength beam-to-column composite joints for seismic applications, *Earthq Eng Struct Dyn 2007*, **36**, 142-61.

[40] M. Latour, V. Piluso, G. Rizzano, Cyclic modeling of bolted beam-to-column connections: component approach, *J Earthq Eng 2011*, **15**, 537-63.

[41] M.J.N. Priestley, D.N. Grant, Viscous damping in seismic design and analysis, *J Earthq Eng 2005*, **9**, 229-55.

[42] E. Brunesi, R. Nascimbene, L. Casagrande , Seismic analysis of high-rise mega-braced frame-core buildings, *Eng Struct 2016*, **115**, 1-17.

[43] E. Brunesi, R. Nascimbene, G.A. Rassati, L. Casagrande , Seismic performance of high-rise steel MRFs with outrigger and belt trusses through nonlinear dynamic FE simulations, *COMPDYN2015, 5th ECCOMAS Thematic Conference on Computational Methods in Structural Dynamics and Earthquake Engineering, Crete Island, Greece 25-27, 2015*.

[44] ABAQUS 6.14 Documentation, *Dassault Systmes Simulia Corp., Providence, RI, USA, 2016*

[45] S. Sivanerupan, J.L. Wilson, E.F. Gad, N.T.K. Lam, Seismic Assessment of Glazed Façade Systems, *Proceedings of the Annual Technical Conference of the Australian Earthquake Engineering Society, Newcastle, 2009*.

[46] A.M. Memari, A. Shirazi, P.A. Kremer, Static finite element analysis of architectural glass curtain walls under in-plane loads and corresponding full-scale test, *Struc Eng and Mech 2007*, **25**(4), 365-382.

[47] J. Kimberlain, L. Carbary, C. D. Clift, P. Hutley, Advanced Structural Silicone Glazing, *International Journal of High-Rise Buildings 2013*, **2**(4), 345-354.

[48] W. Lu, B. Huang, K.M. Mosalam, S. Chen, Experimental evaluation of a glass curtain wall of a tall building, *Earthq Eng Struc Dyn 2016*, **45**, 1185-1205.